Simulation of the emission lines radiated from cataclysmic variables *

Lin He[1,2], Guo-Liang Lü[1] and Yong-Heng Zhao[2]

[1] College of Physical Science and Technology, Xinjiang University, Xinjiang 830046, China;
helin@bao.ac.cn; guolianglv@gmail.com
[2] National Astronomical Observatories, Chinese Academy of Sciences, Beijing 100012, China;
yzhao@lamost.org

Abstract Cataclysmic variables are special celestial bodies because they have particular light curves and spectra. The mechanisms for generating emission lines radiated from dwarf novae in their quiescent phases are studied. We assume that the incident radiation field which is emitted by a hot source (white dwarf and boundary layer) irradiates the gaseous layer evaporated from the accretion disk, and the emission lines are radiated from the gas. We model the fluxes of emission lines by using the photoionization code CLOUDY. Using this method, we input some reasonable parameters and get a series of simulated spectra. In order to find a simulated spectrum which is the best fit to an observed spectrum, we use a cross-correlation method to match them. After the calculation, we use the approximation that the parameters of the simulated spectrum can simulate the observed spectrum. Finally, we learn more about the physical conditions of the system.

Key words: stars: cataclysmic variables — accretion disk: emission lines — emission lines: photoionization

1 INTRODUCTION

A cataclysmic variable (CV) is a close binary system consisting of a white dwarf (WD, the primary) with a low-mass, late-type star (the secondary) which fills its critical Roche surface and transfers matter to the primary. The accreted matter has angular momentum and cannot settle onto the WD, but rather forms a disk around it (Williams 1983). The spectra of cataclysmic variables are dominated by emission lines in the quiescent phase. The emission lines mostly disappear when the secondary star eclipses portions of the accretion disk in cataclysmic variables seen nearly edge-on, indicating that the emitting area for the emission line is constrained to the region of the accretion disk. There are at least three mechanisms that can explain how the emission lines are emitted from the region of the disk. The first mechanism is optically thin emission. In any part of an accretion disk where the vertical optical thickness in the continuum is < 1 but the optical thickness in the lines is significant, an emission spectrum is produced. The importance of this line emission depends on the relative extent of optically thin regions and the spectral region being examined. Having an accretion rate in the low-mass regime, the spectrum radiated by the accretion disk model consists of two parts: The

---

first part is a thermal continuum which is produced by the inner, hotter and optically thick portion of the disk. The second one is a series of emission lines originating from the cooler, outer part of the disk where the gas is optically thick in the lines and thin in the continuum (Williams 1980), and is called chromospheric emission. There are many processes that can heat the optically thin upper layers of the disk's atmosphere. For example, possibilities include turbulence escaping from the disk or magnetic loops arching out of the disk with consequent magneto-hydrodynamic heating of a corona and a downward flow of energy to heat a chromosphere (Shakura & Sunyaev 1973; Liang & Price 1977). The heated gas, which may reach 1×10^8 K, will radiate emission lines (Haardt & Maraschi 1991). The third mechanism is photoionized emission. Energetic photons that are emitted from the central continuum source ionize the gas, and the residual kinetic energy of the photoelectrons heats the gas. The photoelectrons collide with ions and cause internal excitations, which decay to produce collisionally excited emission lines. The electrons eventually recombine with ions and produce recombination lines (Ferland 2003). According to the theory, the integrated fluxes of NOVA CYGNI 1992 have been modeled by means of the photoionization code CLOUDY (Moro-Martín et al. 2001).

We propose that the emission lines in cataclysmic variables are more generally formed from a photoionization mechanism. Then by means of the photoionization code CLOUDY, we simulate the process of producing the emission lines. The incident radiation passes through the gas, which produces emergent spectra. One of the simulated spectra which is the best fit to an observed spectrum can provide some physical parameters describing the observed spectrum.

The layout of this paper is as follows: Section 2 contains a description of the simulated spectra and parameters that enter the calculation. The best match and analysis are given in Section 3. The last section is for the discussion.

2 THE PHOTOIONIZATION MODEL

We use the photoionization model to explain the mechanism of emitting emission lines from CVs. It is essential to assume that there is a gaseous layer on the accretion disk, which has uniform density and constant temperature. The great bulk of photoionizing radiation is produced at the central source, including the WD and boundary layer. A variable mixture of soft X-ray and EUV radiation from a region including the boundary layer illuminates the gaseous layer which we call the chromosphere. The reason why emission lines are produced from the disk is that the chromosphere is photoionized by the underlying thermal source, and the electrons finally recombine with ions and produce recombination lines. The whole process is equivalent to a high energy photon being transformed into two or more low energy photons. The results for the shape of the energy distribution depend on many factors: the temperature and luminosity of the central source (assumed to be a blackbody) (Moro-Martín et al. 2001) and those describing the characteristics of the chromosphere, for example, the hydrogen density, radius, thickness and chemical composition.

The spectra were modeled using the photoionization code CLOUDY (Ferland 2011). The model can solve the equations describing the thermal and statistical equilibrium for the chomosphere of the accretion disk which is photoionized by a central hot source. Based on the code CLOUDY, we simulate the process of producing the emission lines. The incident radiation passes through the gas, which produces emergent radiation. Analyzing this emergent spectrum can provide information about the hydrogen density, temperature, abundances of the elements, and pressure of the chromosphere. In addition, these parameters tell us much about the chromosphere's history and characteristics of the central source (Ferland 2003).

2.1 Temperature and Luminosity of the Central Source

In our model, the temperature of the central source is made up of two parts. The temperature of the WD contributes the first part. According to well-determined measurements, the mean temperatures

are 50 000 K for nova-like variables, 19 200 K for dwarf novae and 13 500 K for polars, which are all higher than the mean value of 10 000 K for DA WDs (Sion 1984). The second contribution comes from the boundary layer which is the region where gas moving at Keplerian velocities in the disk is decelerated to match the surface velocity of the WD. We assume that the boundary layer is optically thick and the luminosity that is deposited must diffuse through a distance H. Thus, the effective temperature of the boundary layer for a non-rotating primary is given by

$$4\pi R_{\mathrm{WD}} H \sigma T_{\mathrm{BL}}^4 \simeq \frac{GM_{\mathrm{WD}}\dot{M}(d)}{2R_{\mathrm{WD}}}.$$ (1)

According to the most complete optically thick two-dimensional models, the result shows that $T_{\mathrm{BL}} > 2.8 \times 10^5$ K and there is no pronounced wind (Kley & Hensler 1987; Kley 1989a,b,c, 1990, 1991). There is observational evidence of strong stellar winds from the inner disk or boundary layer in systems with a high accretion rate, which has $T_{\mathrm{BL}} \leq 1 \times 10^5$ K. In our model, we combine the two parts into a whole. We take the medial temperatures as the temperature of the central source and the corresponding numerical values are set as: 50 000, 60 000, 70 000, 80 000 and 90 000 K.

Gravitational energy will be released when the accreted matter falls onto the surface of the WD; at the same time, the luminosity is produced from accretion, which is given by

$$L = \frac{GM_{\mathrm{WD}}\dot{M}(d)}{R_{\mathrm{WD}}},$$ (2)

where $R_{\mathrm{WD}} = 5 \times 10^8$ cm and $M_{\mathrm{WD}} = 1 M_\odot$; the accretion rate of the dwarf nova is about $2\times10^{-11}-5\times10^{-10} M_\odot \mathrm{yr}^{-1}$ during quiescence (Warner 1995). We take $1\times10^{-11}M_\odot \mathrm{yr}^{-1}$ as the accretion rate in our model. The resulting value of luminosity for the central source is 10^{32} erg s^{-1}.

2.2 Radius, Thickness, Hydrogen Density, Chemical Abundances and Geometry of the Chromosphere

When the chromosphere is formed on the disk, the distance between the inner and outer radius is almost equivalent to distance from the inner radius to the disk. The radius of the WD is about 10^{8-9} cm (Camenzind 2007), which has the same order of magnitude as the inner radius of the disk, but the latter is larger than the former. The inner radius of the chromosphere takes values of 10^8 cm, $10^{8.5}$ cm and 10^9 cm. Because of the influence of the companion's gravity, the expansion of the outside radius of the accretion disk cannot be unlimited and should have a maximum outer radius (Warner 1995). Paczynski computed single particle orbits and tabulated the maximum radius vector of the last nonintersecting orbit (Paczynski 1977). The following equation can approximate his results

$$\frac{r_d(\mathrm{max})}{a} = \frac{0.60}{1+q}, \quad 0.03 < q < 1.$$ (3)

where a is the distance of the center of mass between the primary star and companion star. q is the mass ratio $M_{\mathrm{primary}}/M_{\mathrm{secondary}}$. a can be expressed as follows

$$a = \sqrt[3]{\frac{P^2}{(4\pi^2)}G(M_1 + M_2)}.$$ (4)

In centimeter-gram-second units, we set $M_1 = M_{\mathrm{primary}} = 1M_\odot$, $M_2 = M_{\mathrm{secondary}} = 0.5M_\odot$ and orbital periods of 3–10 h. Then, the outer radius can reach up to 3×10^{11} cm, so the range of outer radius of the chromosphere in our model is $10^{10-11.4}$ cm. The density of hydrogen in the chromosphere is composed of

$$n(\mathrm{H}) = \left(n(\mathrm{H}^0) + n(\mathrm{H}^+) + 2n(\mathrm{H}^2) + \sum n(\mathrm{H}_{\mathrm{other}})\right) \mathrm{cm}^{-3},$$ (5)

Table 1 Abundances

Element	He	C	N	O	Ne	Na	Mg	Al	Si	S	Ar	Ca
Abundance	−1.50	−6.15	−6.37	−5.70	−6.00	−7.10	−6.35	−7.42	−6.29	−6.74	−8.90	−7.97

Element	Fe	Ni	Li	P	K	Cl	Sc	Ti	V	Cr	Mn
Abundance	−6.00	−7.19	−9.00	−7.00	−7.00	−10.00	−8.00	−8.00	−8.00	−7.00	−7.00

where the density is regarded as a free parameter in the model and its values are 9.5, 10, 10.5 and 11 (log of hydrogen density in $10^{-3}\,\mathrm{cm}^{-3}$). The abundance of the chromosphere is referred to as solar composition and we made some changes on the basis of observed spectra. According to the observed spectra, the composition of He, C, N, O, Ne, Na, Al, Si, S, Ar, Ca, Fe and Cl are different from the solar composition. The abundances are shown in Table 1.

In the model, we assume that the geometry of the chromosphere is cylindrical and is distributed on the upper and lower surfaces of the thin disk. Its half-height is 10^8 cm. With these parameters, we compute a series of simulated spectra in order to match the observed spectra and simulate the conditions where they are emitted.

3 MATCH WITH OBSERVED SPECTRA

3.1 Comparison of Emission Line Intensity

We compared observed spectra with simulated spectra in terms of their characteristic emission lines to find the best match to the simulated spectra. In the observed spectrum, ten lines were selected for their intensity relative to Hβ, which are: He 3889, H 3970, H 4102, H 4340, He 4471, He 6678, He 5876, He 7065, H 6563 and H 4861. Meanwhile, the ten relative values are represented by b_j. We perform the same processing of the simulated spectra and use a_{ij} to represent the jth line in the ith simulated spectrum. The best match is given by

$$\min W_i = \sqrt{\sum_j \left[a_{ij} - b_j\right]^2}.\qquad(6)$$

With Equation (6), we can find a simulated spectrum that best fits an observed spectrum.

3.2 Comparison Using the Continuum

In order to increase the accuracy of the fit, we not only match the characteristic emission lines but also fit the continuum. Sometimes, it is not reliable if we only depend on the similarity of emission line intensity to find the best matching spectrum, so the continuum is added to derive a more reliable fit between the observed spectra and the simulated ones. We use the method of cross correlation to find the best matching simulated spectrum. SDSS J101037.05+024915.0 (Abazajian et al. 2009), SDSS J230351.64+010651.0 (Szkody et al. 2002) and SDSS J102517.94+430221.2 (Szkody et al. 2005) are taken as the observed spectra and the results of fitting are shown in Figures 1–3. The best fitting parameters are shown in Table 2.

4 DISCUSSION

As is shown in the figures, the simulated spectra show a good match with the observed ones. However, in Figures 2 and 3, the Hα lines are not fitted very well, because the two observed spectra have the obvious characteristic of a flat Balmer decrement. Williams found that the Balmer decrement will depend on the density of the disk in non-LTE models for the optically thin region at the

Table 2 Model Parameters

Observed Spectra	$\log T^b$	$\log n_{\mathrm{H}}^c$	$\log R_{\mathrm{in}}^d$	$\log R_{\mathrm{out}}^e$
SDSS J101037.05+024915.0	4.78	11.00	8.50	10.70
SDSS J230351.64+010651.0	4.70	11.00	8.50	10.60
SDSS J102517.94+430221.2	4.70	11.00	8.50	10.50

[a] Luminosity of the central source=10^{32} erg s^{-1}; [b] Blackbody temperature (K); [c] Hydrogen density (cm^{-3}); [d] Inner radius (cm); [e] Outer radius (cm).
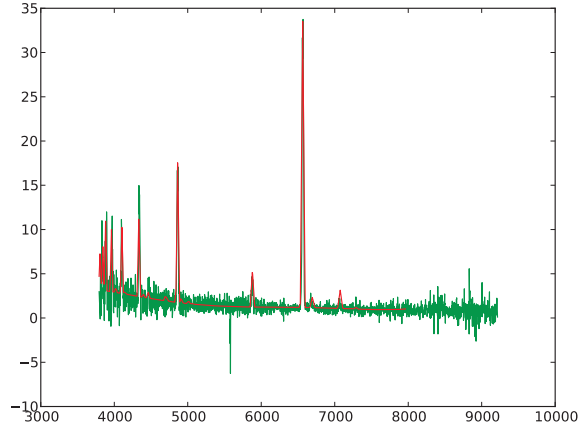
Fig. 1 Comparison between the observed (*green line*) and the synthetic (*red line*) spectra of SDSS J101037.05+024915.0. The x-axis and y-axis are the wavelength and the flux relative to the value of $\lambda5001$, respectively.
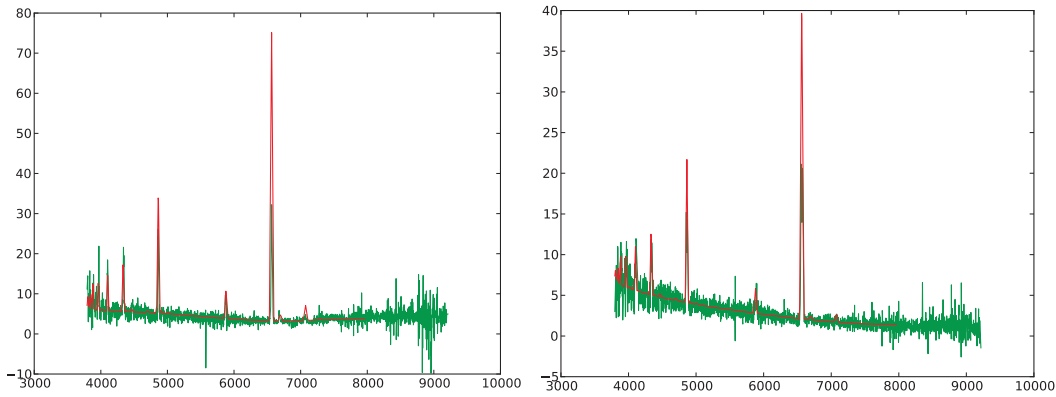
Fig. 2 Observed spectrum is SDSS J230351.64 +010651.0.

Fig. 3 Observed spectrum is SDSS J102517.94 +430221.2.

outer edge of a cataclysmic variable's accretion disk (Williams et al. 1988). It is confirmed that SDSS J230351.64+010651.0 is a dwarf nova (Szkody et al. 2002), but the other two objects are not classified in detail. We conjecture that the two objects are also dwarf novae because their parameters are similar to SDSS J230351.64+010651.0. In the next work, we will focus on considering the impact of

the density of the disk and increase the number of calculated spectra, in order to improve the accuracy of simulating the observed spectra. In the future, it will be possible to differentiate varieties of CVs according to the parameters given by our model or give a new classification of CVs depending on the statistical law of a large numbers for fitting the observed spectra and the simulated ones.

References

Abazajian, K. N., Adelman-McCarthy, J. K., Agüeros, M. A., et al. 2009, ApJS, 182, 543

Camenzind, M. 2007, Compact Objects in Astrophysics: White Dwarfs, Neutron Stars, and Black Holes (Springer Press)

Ferland, G. J. 2003, ARA&A, 41, 517

Ferland, G. J. 2011, Hazy, A Brief Introduction to Cloudy (University of Kentucky), *http://data.nublado.org/cloudy_releases/c10/*

Haardt, F., & Maraschi, L. 1991, ApJ, 380, L51

Kley, W., & Hensler, G. 1987, A&A, 172, 124

Kley, W. 1989a, A&A, 208, 98

Kley, W. 1989b, A&A, 222, 141

Kley, W. 1989c, in NATO ASIC Proc. 290: Theory of Accretion Disks, ed. F. Meyer, 289

Kley, W. 1990, in Accretion-Powered Compact Binaries, ed. C. W. Mauche (Cambridge Univ. Press), 301

Kley, W. 1991, A&A, 247, 95

Liang, E. P. T., & Price, R. H. 1977, ApJ, 218, 247

Moro-Martín, A., Garnavich, P. M., & Noriega-Crespo, A. 2001, AJ, 121, 1636

Paczynski, B. 1977, ApJ, 216, 822

Shakura, N. I., & Sunyaev, R. A. 1973, A&A, 24, 337

Sion, E. M. 1984, ApJ, 282, 612

Szkody, P., Anderson, S. F., Agüeros, M., et al. 2002, AJ, 123, 430

Szkody, P., Henden, A., Fraser, O. J., et al. 2005, AJ, 129, 2386

Warner, B. 1995, Cataclysmic Variable Stars, in Cambridge Astrophysics Series (Cambridge : Cambridge Univ. Press), 28

Williams, R. E. 1980, ApJ, 235, 939

Williams, G. 1983, ApJS, 53, 523

Williams, G. A., & Shipman, H. L. 1988, ApJ, 326, 738